

OPEN ACCESS

Optical thin film metrology for optoelectronics

To cite this article: Peter Petrik 2012 *J. Phys.: Conf. Ser.* **398** 012002

View the [article online](#) for updates and enhancements.

You may also like

- [In situ characterization of Fischer–Tropsch catalysts: a review](#)
N Fischer and M Claeys
- [Scatterometry—fast and robust measurements of nano-textured surfaces](#)
Morten Hannibal Madsen and Poul-Erik Hansen
- [Room Temperature Photoluminescence and Raman Characterization of Interface Characteristics of SiN/SiO₂/Si Prepared under Various Deposition Techniques and Conditions](#)
Woo Sik Yoo, Byoung Gyu Kim, Seung Woo Jin et al.



ECS
The
Electrochemical
Society
Advancing solid state &
electrochemical science & technology

DISCOVER
how sustainability
intersects with
electrochemistry & solid
state science research

Optical thin film metrology for optoelectronics

Peter Petrik^{1,2,3}

¹ Fraunhofer Institute for Integrated Systems and Device Technology, Schottkystrasse 10, 91058 Erlangen, Germany

² Research Centre for Natural Sciences - Institute for Technical Physics and Materials Science, Konkoly Thege Rd. 29-33, 1121 Budapest, Hungary

³ Doctoral School of Molecular- and Nanotechnologies, Faculty of Information Technology, University of Pannonia, Egyetem u. 10, Veszprem, H-8200, Hungary

E-mail: peter.petrik@ttk.mta.hu

Abstract. The manufacturing of optoelectronic thin films is of key importance, because it underpins a significant number of industries. The aim of the European joint research project for optoelectronic thin film characterization (IND07) in the European Metrology Research Programme of EURAMET is to develop optical and X-ray metrologies for the assessment of quality as well as key parameters of relevant materials and layer systems. This work is intended to be a step towards the establishment of validated reference metrologies for the reliable characterization, and the development of calibrated reference samples with well-defined and controlled parameters. In a recent comprehensive study (including XPS, AES, GD-OES, GD-MS, SNMS, SIMS, Raman, SE, RBS, ERDA, GIXRD), Abou-Ras et al. (Microscopy and Microanalysis 17 [2011] 728) demonstrated that most characterization techniques have limitations and bottle-necks, and the agreement of the measurement results in terms of accurate, absolute values is not as perfect as one would expect. This paper focuses on optical characterization techniques, laying emphasis on hardware and model development, which determine the kind and number of parameters that can be measured, as well as their accuracy. Some examples will be discussed including optical techniques and materials for photovoltaics, biosensors and waveguides.

1. Introduction

Although the development of optoelectronic materials strongly depends on accurate and reliable metrologies, it has recently been shown that in spite of high sensitivities, large deviations (exceeding the error bars) can be obtained between the results of elemental depth profiling performed by different methods (see figure 1 from Ref. [1]). This fact puts emphasis on proper modeling, calibration, and verification for all metrologies. While the agreement between the profiles shown in figure 1 are far from being perfect, the situation is even worse taking into account that the total amount of Ga over the whole layer has been normalized to a reference value determined by X-ray fluorescence.

Most of the methods taking part in the study are summarized in Table 1. In the first group, reliable optical models have to be found for the proper depth profiling. In the second group, the sputter rate has to be calibrated - e.g. by reference measurements with ellipsometry. The last group using cross sections consists of the mostly direct methods. However, the agreement is not perfect in this case either. Though depth resolutions of 1 nm or even below (in case of ellipsometry) can be reached, lateral resolution is a problem for the first two groups of Table

1. Even for ellipsometry, the best lateral resolutions are in the range of approximately 50 μm . The sensitivity is in most cases at or below 1 %. However, as the comparison in figure 1 reveals, the accuracy of (and agreement between) depth profiles is worse than these specified values for most of the methods.

From the huge field of metrologies optical techniques will be in the focus of this short review. Examples of development of instrumentation and modeling for photovoltaics and liquid crystal modulated waveguide sensorics will be presented.

Table 1. Measurement techniques for the determination of elemental depth distribution. The listed parameters are typical values used in the study of Abou-Ras et al. [1]. RBS: Rutherford Backscattering Spectrometry; ERDA: Elastic Recoil Detection Analysis; GIXRD: Grazing Incidence X-Ray Diffraction; SNMS: Sputtered Neutral Mass Spectrometry; SIMS: Secondary Ion Mass Spectrometry; XPS: X-Ray Photoelectron Spectrometry; AES: Auger Electron Spectrometry; GD-OES: Glow-Discharge Optical Emission Spectrometry; TEM-EDX: Energy-Dispersive X-Ray Spectrometry in a Transmission Electron Microscope.

Method	Depth resolution (nm)	Sensitivity (at. %)
Depth profiling by modeling		
Ellipsometry	1	0.2-2
RBS	10	1
ERDA	10	10^{-4}
GIXRD	100	1
Depth profiling by sputtering		
SNMS	1	0.05
SIMS	4	$10^{-7} - 10^{-3}$
XPS	1-10	0.1
AES	10	0.3
GD-OES	3-100	$10^{-5} - 10^{-3}$
Raman depth profiling	100	1
Depth profiling using cross section		
Scanning Auger	1	3
TEM-EDX	Specimen thickness	0.5
SEM-EDX	Few 100	3

2. Instrumentation

Probably the most significant research field within optoelectronics is photovoltaics. Low cost and effective manufacturing of solar panels requires large area processing, most of the steps being thin film deposition. Taking advantage of its sensitivity, speed and non-destructive manner, ellipsometry is an attractive tool for in line monitoring of thin film properties.

The research group of M. Fried at the MFA developed a patented mapping ellipsometry concept for large area thin film characterizations [2–6]. The basic idea is the use of a divergent light source. Figure 2 shows the construction (left), the schematics (middle) and the beam path (right) of the mapping ellipsometer. This way, a large area can be illuminated, limited only by the geometrical constraints of the deposition or monitoring chamber. In our application at the Center for Photovoltaics Innovation and Commercialization at the University of Toledo this area is several dm^2 . This new version applies a spherical mirror to collect light to the detector.

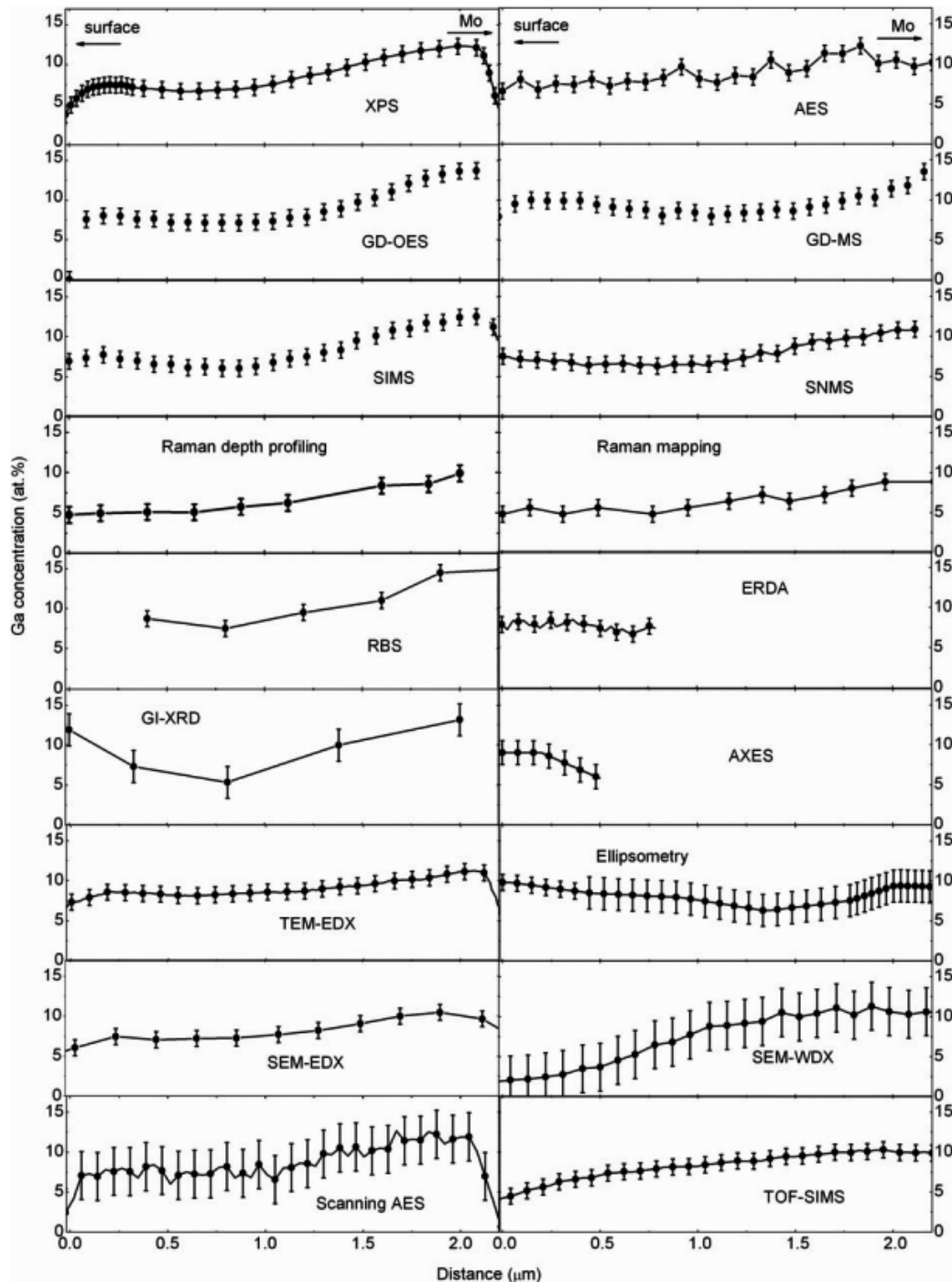


Figure 1. Ga distributions in $\text{Cu}(\text{In,Ga})\text{Se}_2$ measured by different techniques. The surface is at distance zero. The lines are guides for the eyes. The error bars are estimated individually for each technique. Note that the differences between the different techniques are in a lot of cases larger than the error bars [1]. The used techniques are summarized in Table 1, except for GD-MS (Glow-Discharge Mass Spectrometry), AXES (Angle-Dependent Soft X-ray Emission Spectroscopy), SEM-WDX (SEM-Wavelength-Dispersive X-ray Spectrometry), and TOF-SIMS (Time-of-Flight SIMS). [Reprinted from *Microscopy and Microanalysis* 17, Abou-Ras et al., Comprehensive comparison of various techniques for the analysis of elemental distributions in thin films, 728 (2011). Copyright (2011) Microscopy Society of America.]

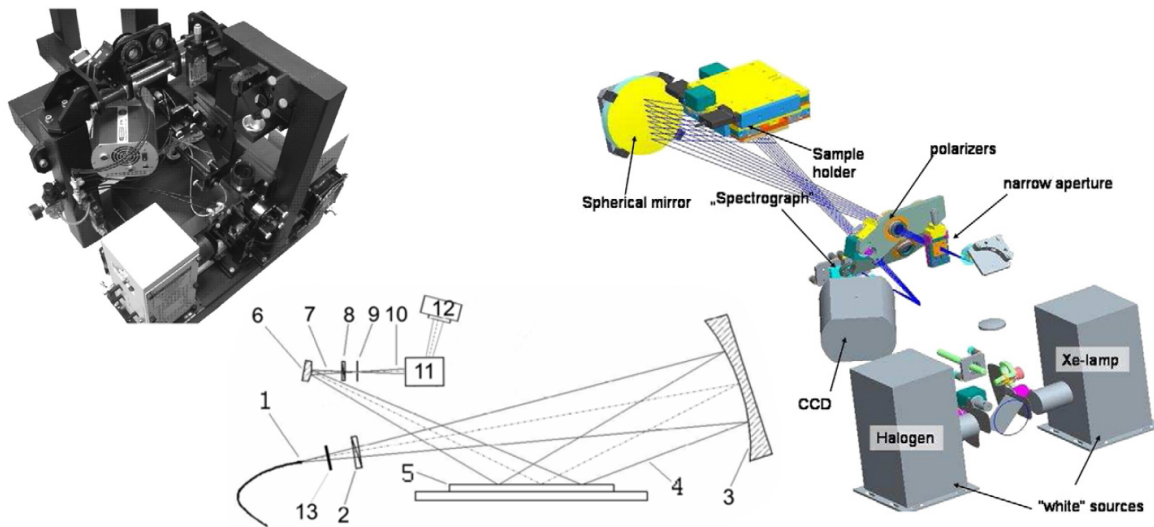


Figure 2. Expanded beam mapping ellipsometry. The prototype, located in the Center for Photovoltaics Innovation and Commercialization at University of Toledo (Ohio) can be seen on the left-hand side. The working principle and the main components are shown in the middle ([1] point source; [2] polarizer; [3] spherical mirror; [4] non collimated beam; [5] sample; [6] cylindrical mirror; [7] corrected beam; [8] analyzer; [9] pinhole; [10] beam after pinhole; [11] corrector-disperser optics; [12] ccd detector; [13] rectangular (narrow) aperture), whereas the exploded drawing on the right-hand side shows the beam-guiding in the chamber and the main components of the arrangement (see [4]).

The image on the CCD is created by a pin hole. In this spectroscopic version one index of the CCD is the spectral information and the other index is the spatial information along a line. 2D images can be taken by moving the sample perpendicular to that line. Note that in a roll-to-roll production this movement is already part of the manufacturing process. This allows an easy integration of the tool as an in line process monitor [7].

Following the first demonstration of the concept [8], there has been a remarkable progress in the field of label-free optical biosensor development [9–11]. These sensors utilize the fact that the propagation of light in waveguides sensitively depend on the refractive index difference at the waveguide surface (i.e. between the waveguide and the ambient - the latter being e.g. a protein solution). The light is coupled into the waveguide from the substrate, using a grating. The coupling angle sensitively depends on the above mentioned difference, which allows the detection of refractive index changes down to 10^{-5} . Consequently, also proteins and other objects adsorbed to the surface can be detected with high sensitivity. In the research group of R. Horvath a new sensor concept has been developed that avoids using moving parts by measuring the coupling angle (see e.g. Ref. [12]), but also makes the sensor highly integrable [13, 14]. A schematic drawing of the device is shown in figure 3. The tool utilizes two coupling gratings, whereas one of the light beams is modulated using a liquid crystal modulator. The phase shift sensitively depends on the refractive index, i.e. the number of molecules attached to the surface of the waveguide.

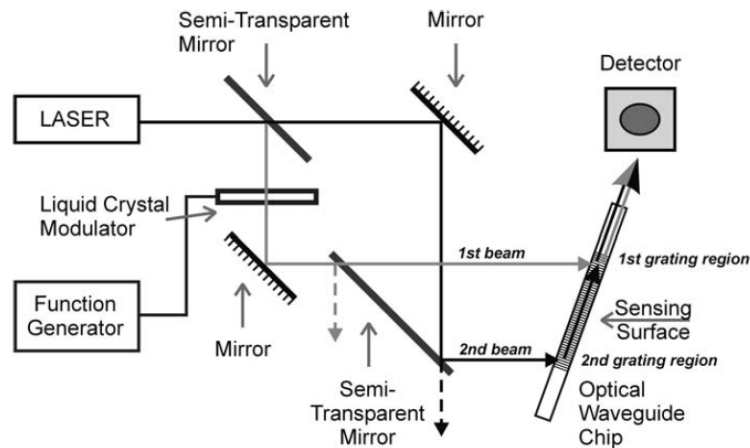


Figure 3. Grating coupled interferometer. The gray and black lines represent the reference and measurement arms of the interferometer, respectively [14]. [Reprinted from Applied Physics B 97, Kozma et al., Grating coupled interferometry for optical sensing, 5 (2009). Copyright (2009) Springer Verlag.]

3. Evaluation and modeling

The fairly large deviation between the metrologies shown in figure 1 is to a great extent a question of proper modeling. A large part of optical techniques is indirect in a sense that derived layer properties can only be determined if a suitable and reliable optical model exists for the structure. The test, whether a model is acceptable is not straightforward, although a couple of rules can be set to create reliable models (see Ref. [15] or page 2 of Ref. [16]).

The optical modeling of optoelectronic thin films is usually a complex problem for at least two reasons: (i) the electronic band structure and the related dielectric function is strongly dependent upon the preparation conditions, which rules out almost completely the use of reference dielectric functions, hence requires the application of analytical models; (ii) thin films created by the most usual (mostly deposition-related) techniques are only in exceptional cases uniform to the scale of precision of the most sensitive optical techniques like ellipsometry. In most cases at least the surface nanoroughness and an interface layer to the substrate have to be taken into account [16–19]. It can be shown that the optical modeling of one of the most frequently applied transparent conductive oxide (TCO) materials, Indium-Tin Oxide (ITO) is also a complex process [20–27], in which special care has to be taken for the modeling of vertical non-uniformity [28]. Most significant improvement was obtained by introducing a surface roughness layer as well as upper and bottom sublayers [28].

ZnO is also a key material for optoelectronic applications [29], used e.g. as TCO in photovoltaics to substitute ITO. The measurement of its optical properties is still a challenging task [30,31]. A typical dielectric function of a low-resistance ZnO film is shown in figure 4 as a composition of different oscillators corresponding to excitonic and other electronic transitions [32]. The significance of the interpretation of optical spectra lies with the fact that the optical properties (especially at photon energies around the band gap) correlate with crucial electronic properties as e.g. the specific resistance [30,33]. Figure 5 reveals a fairly good correlation between the optically measured exciton strength and the specific resistance. An even better correlation was shown by Hwang et al. between the band gap (also studied in Ref. [30]) and the carrier concentration for sputter deposited and annealed ZnO:Al films [33].

A possible strategy for the model-independent measurement of the dielectric function of ZnO

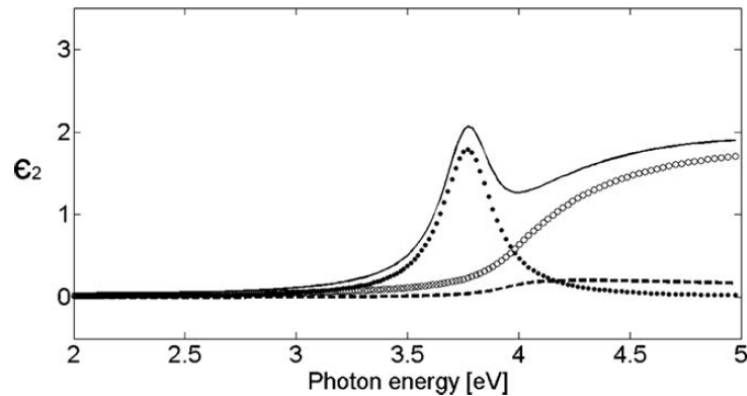


Figure 4. Typical dielectric function of a sputter-deposited ZnO:Al sample with low specific resistance from Ref. [30]. Solid line is the sum of the individual oscillators shown by the circled, dotted, and dashed lines. The dotted and dashed lines show the discrete-exciton and the continuum-exciton oscillators, respectively (see further details in Ref. [30]). [Reprinted from Applied Surface Science 255, Major et al., Optical and electrical characterization of aluminium doped ZnO layers, 8907 (2009). Copyright (2009) Elsevier.]

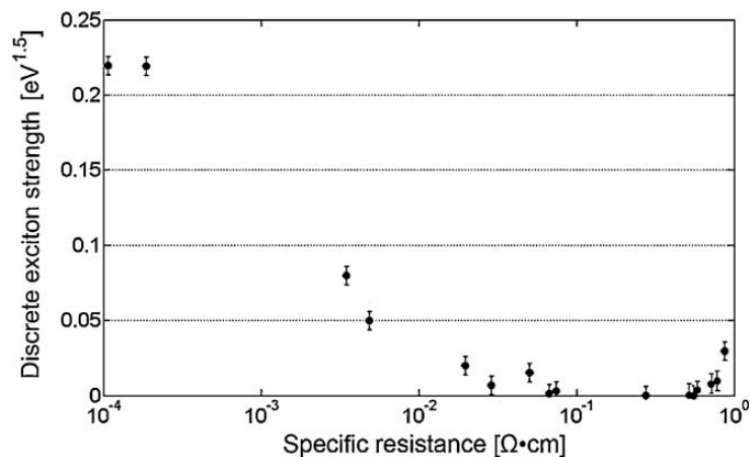


Figure 5. Discrete exciton strength parameter as the function of specific resistance [30]. [Reprinted from Applied Surface Science 255, Major et al., Optical and electrical characterization of aluminium doped ZnO layers, 8907 (2009). Copyright (2009) Elsevier.]

in a wide spectral range (as for most non-zero gap materials) is to determine the layer thickness by fitting the spectra in a relatively narrow transparent wavelength range. Under this conditions the Cauchy model can usually be applied, neglecting the absorption (i.e. only the real part of the refractive index will be fitted using a polynomial with fit parameters A, B, and C as follows: $n = A + B/\lambda^2 + C/\lambda^4$, where λ denotes the wavelength). As soon as the thickness is known, the real and imaginary parts of the refractive index (n and k) or dielectric function (ϵ_1 and ϵ_2) can be determined for each wavelength independently, because two ellipsometric angles (Ψ and Δ) are measured at each angle of incidence, whereas the number of unknown model parameters is only two: n and k . This leads to a model-independent point-by-point determination of the

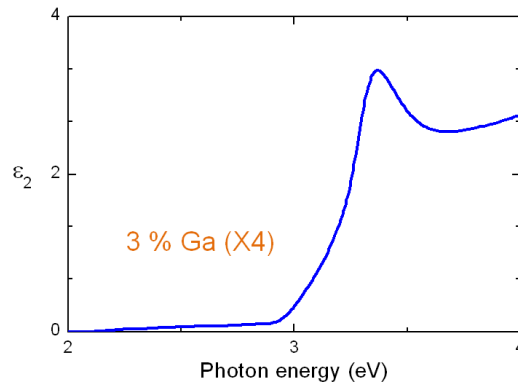


Figure 6. Imaginary part of the dielectric function of a sputter-deposited GaInZnO layer with nominally 3 and 6 % Ga and In contents, respectively, using point-by-point determination based on the layer thickness fitted in the transparent spectral region.

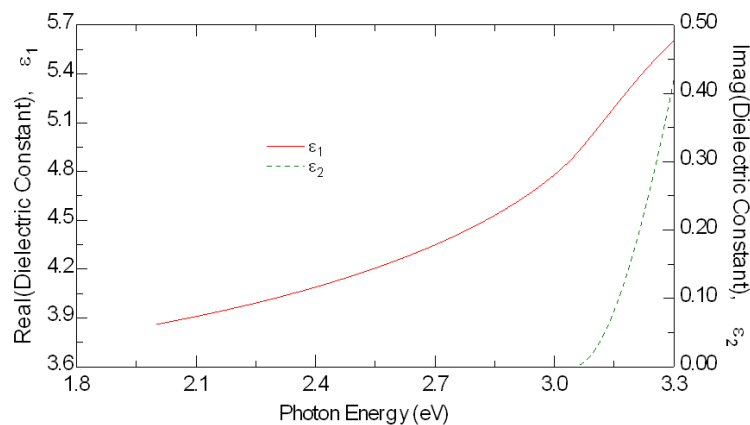


Figure 7. Typical dielectric function of a sputter-deposited GaInZnO film evaluated using the Tauc-Lorentz model.

dielectric function as shown in figure 6. Note the good agreement between the point-by-point (figure 6) and the oscillator (figure 4) approach. By checking the effect of whether the proper layer thickness was chosen, or most importantly, the effect of layer thickness to the results, the ϵ_2 spectrum of figure 6 was found to be stable. In case of Si oscillations may appear when using a wrong layer thickness [34].

To analyze the band gap region, (or more specifically: to obtain numerical gap parameters) the Tauc-Lorentz model can also be used, though in a limited spectral range (see figure 7). This model can be used to fit the decay of ϵ_2 at the band edge, assuming a quadratic behavior. The equation of the Tauc-Lorentz model can be obtained by multiplying the quadratic near-edge Tauc function [35,36] by a Lorentz oscillator [37], which finally takes the form $k = A(E - E_g)^2 / (E^2 - BE + C)$, where E denotes the photon energy, A , E_g , B , and C are the amplitude, gap, strength, and broadening parameters. From this model the energy of the band gap and the amplitude of the excitonic oscillator at the band edge can directly be determined.

Waveguides are basic building blocks of potential integrated optic amplifiers and lasers, also applied in biosensors mentioned above. Ion implantation is a tool with remarkable capabilities

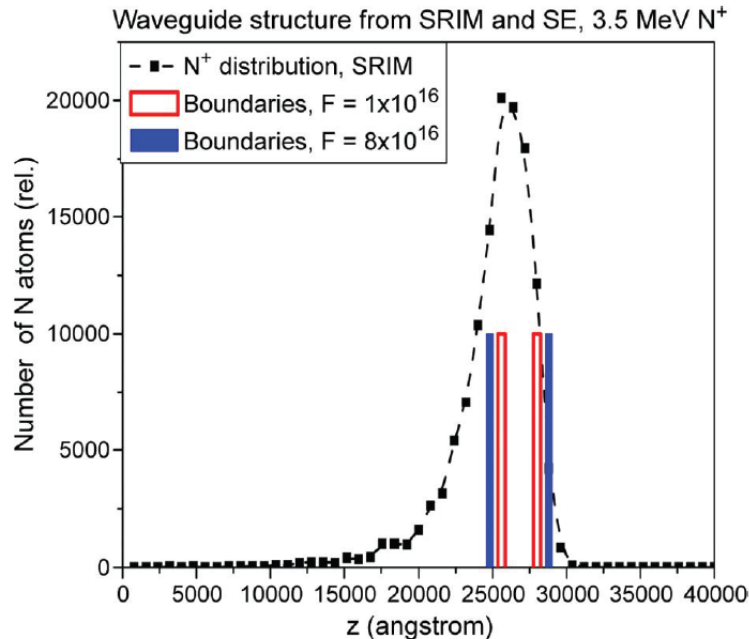


Figure 8. Depth position of the waveguiding layer determined by ellipsometry and SRIM (Stopping and Range of Ions in Matter) [39]. [Reprinted from IEEE Photonics Journal 4, Bányász et al., MeV Energy N⁺-Implanted Planar Optical Waveguides in Er-Doped Tungsten-Tellurite Glass Operating at 1.55 μm , 721 (2012). Copyright (2012) IEEE.]

also for waveguide fabrication [38,39]. Waveguides prepared by 3.5-MeV N⁺ implantation into Er:Te glasses have been demonstrated by Banyasz et al. [39], characterized by M-line spectroscopy and ellipsometry. A fluence-dependent change of refractive index in the range of 0.04-0.09 have been revealed by ellipsometry in a waveguide layer approximately 2.5 micron below the implanted Er:Te glass surface. A three-layer model, consisting of (1) a surface nanoroughness layer, (2) a non-damaged surface layer (with a thickness of about 2.5 micron) and (3) a buried waveguide layer in the stopping region of the ions (as verified by the SRIM [Stopping and Range of Ions in Matter] program [40]) was used with Cauchy parametrizations in layers (2) and (3). The surface roughness layer was an effective medium mixture of the ambient and the underlying non-damaged Er:Te glass with a volume fraction fixed at 50 %. The position of the buried waveguide layer determined by ellipsometry is depicted in figure 8 together with the N⁺ distribution calculated by SRIM.

4. Conclusions

It was shown in this brief review that modeling, calibration and verification is still a crucial issue for reliable metrology. Examples have been presented for the improvement of instrumentation and modeling for a couple of optical techniques and materials. The demand for the characterization of layers and structures with ever increasing complexity requires the construction of complicated optical models with numerous fit parameters. However, the importance of the verification of results has to be pointed out.

Acknowledgments

Support from the European Community's Seventh Framework Program, European Metrology Research Program (EMRP), ERA-NET Plus, under Grant Agreement No. 217257 (the EMRP is jointly funded by the EMRP participating countries within EURAMET and the European Union) as well as from the National Development Agency grant TMOP-4.2.2/B-10/1-2010-0025 and OTKA grant Nr. K81842 is greatly acknowledged.

References

- [1] Abou-Ras D, Caballero R, Fischer C H, Kaufmann C A, Lauer mann I, Mainz R, Mönig H, Schöpke A, Stephan C, Streeck C, Schorr S, Eicke A, Döbeli M, Gade B, Hinrichs J, Nunney T, Dijkstra H, Hoffmann V, Klemm D, Efimova V, Bergmaier A, Dollinger G, Wirth T, Unger W, Rockett A A, Perez-Rodriguez A, Alvarez-Garcia J, Izquierdo-Roca V, Schmid T, Choi P P, Müller M, Bertram F, Christen J, Khatri H, Collins R W, Marsillac S and Kötschau I 2011 *Microsc. Microanal.* **17** 728
- [2] Juhasz G, Horvath Z, Major C, Petrik P, Polgar O and Fried M 2008 *Phys. Stat. Solidi C* **5** 1081
- [3] Major C, Juhasz G, Petrik P, Horvath Z, Polgar O and Fried M 2009 *Vacuum* **84** 119
- [4] Fried M, Juhasz G, Major C, Petrik P, Polgár O, Horváth Z and Nutsch A 2011 *MRS Proceedings* **1323** 157
- [5] Fried M, Juhasz G, Major C, Nemeth A, Petrik P, Polgar O, Salupo C, Dahal L R and Collins R W 2011 *Thin Solid Films* **519** 2730
- [6] Nemeth A, Attygalle D, Dahal L R, Aryal P, Huang Z, Salupo C, Petrik P, Juhasz G, Major C, Polgar O, Fried M, Pecz B and Collins R W 2011 *MRS Proceedings* **1321** 267
- [7] Fried M, Juhasz G, Major C, Nemeth O P A, Petrik P, Dahal L R, Huang Z, Attygalle D, Shan A, Chen J, Podraza N J and Collins R W Fast imaging/mapping spectroscopic ellipsometry for large area samples unpublished
- [8] Tiefenthaler K and Lukosz W 1985 *Thin Solid Films* **126** 205
- [9] Ramsden J J 1993 *Phys. Rev. Lett.* **71** 295
- [10] Horvath R, Pedersen H, Skivesen N, Selmeçzi D and Larsen N B 2003 *Opt. Lett.* **28** 1233
- [11] Horvath R, Cottier K, Pedersen H C and Ramsden J J 2008 *Biosens. Bioelectron.* **24** 799
- [12] Horvath R, Skivesen N and Pedersen H C 2004 *Appl. Phys. Lett.* **84** 4044
- [13] Cottier K patent published on September 18, 2008 Integrated optical sensor wO2008110026
- [14] Kozma P, Hamori A, Cottier K, Kurunçzi S and Horvath R 2009 *Appl. Phys. B* **97** 5
- [15] Aspnes D E 1982 *Thin Solid Films* **89** 249
- [16] Petrik P 2012 *Characterization of polysilicon thin films using in situ and ex situ spectroscopic ellipsometry* Ph.D. thesis Technical University of Budapest http://petrik.ellipsometry.hu/petrik_phd.pdf
- [17] Petrik P, Lohner T, Fried M, Biró L P, Khánh N Q, Gyulai J, Lehnert W, Schneider C and Ryssel H 2000 *J. Appl. Phys.* **87** 1734
- [18] Petrik P, Fried M, Vazsonyi E, Basa P, Lohner T, Kozma P and Makkai Z 2009 *J. Appl. Phys.* **105** 024908
- [19] Petrik P 2012 *Nanocrystals - Synthesis, Characterization and Applications* ed Neralla S (<http://dx.doi.org/10.5772/48732>: InTech)
- [20] Fukarek W and Kersten H 1994 *J. Vac. Sci. Technol. A* **12** 523
- [21] Woollam J A, McGahan W A and Johs B 1994 *Thin Solid Films* **241** 44
- [22] Synowicki R 2002 *Thin Solid Films* **20** 37
- [23] Dobrowolski J, Li L and Hilfiker J 1999 *Applied Optics* **38** 4891
- [24] Losurdo M, Giangregorio M, Capezzuto P, Bruno G, Rosa R D, Roca F, Summonte C, Plá J and Rizzoli R 2002 *J. Vac. Sci. Technol.* **20** 37
- [25] Jung Y S 2004 *Thin Solid Films* **467** 36
- [26] Kim J K, Chhajed S, Schubert M F, Schubert E F, Fischer A J, Crawford M H, Cho J, Kim H and Sone C 2008 *Advanced Materials* **20** 801
- [27] Tejo-Cruz C, Mendoza-Galván A, López-Beltrán A M and Garcia-Jimenez M 2009 *Thin Solid Films* **517** 4615
- [28] Lohner T, Kumar K J, Petrik P, Subrahmanyam A and Bársony I Analyses of optical thickness and refractive index of magnetron sputtered ito thin films: comparison of reflectometry and variable angle spectroscopic ellipsometry techniques unpublished
- [29] Özgür U, Alivov Y I, Liu C, Teke A, Reshchikov M A, Dogan S, Avrutin V, Cho S J and Morkoc H 2005 *J. Appl. Phys.* **98** 041301
- [30] Major C, Nemeth A, Radnoczi G, Czigany Z, Fried M, Labadi Z and Barsony I 2009 *Appl. Surf. Sci.* **255** 8907
- [31] Gupta R K, Cavas M and Yakuphanoglu F 2012 *Spectrochimica Acta Part A: Molecular and Biomolecular Spectroscopy* **95** 107

- [32] Yoshikawa H and Adachi S 1997 *Japanese Journal of Applied Physics* **36** 6237
- [33] Hwang Y, Kim H and Um Y 2012 *Current Applied Physics* **currently in press**
- [34] Aspnes D E, Studna A A and Kinsbron E 1984 *Phys. Rev. B* **29** 768
- [35] Tauc J, Grigorovici R and Vancu A 1966 *Phys. Status Solidi* **15** 627
- [36] Tauc J 1969 *Optical Properties of Solids* ed Nudelman S and Mitra S S (New York: Plenum)
- [37] G E Jellison J and Modine F A 1996 *Appl. Phys. Lett.* **69** 371
- [38] Banyasz I, Berneschi S, Khanh N Q, Lohner T, Fried M, Petrik P, Zolnai Z, Lengyel K, Peter A, Watterich A, Nunzi-Conti G, Pelli S and Righini G C 2010 *IOP Conference Series: Materials Science and Engineering* **15** 012027
- [39] Banyasz I, Berneschi S, Brenci M B M, Fried M, Khanh N Q, Lohner T, Conti G N, Pelli S, Petrik P, Righini G C, Speghini A, Watterich A and Zolnai Z 2012 *IEEE Photonics Journal* **4** 721
- [40] Ziegler J F 2004 *Nucl. Instr. Meth. Phys. Res. B* **219** 27 <http://www.srim.org>